Attitude Determination from a Balloon-Borne Radiometer Using Two-Sided Limb Scanning

J. R. DRUMMOND, D. TURNER AND A. ASHTON

Department of Physics, University of Toronto, Toronto, Ontario, Canada M5S 1A7

(Manuscript received 7 November 1984, in final form 1 July 1985)

ABSTRACT

The determination of the horizontal attitude of a balloon-borne, infrared, limb-scanning radiometer is discussed. In particular, the relationship between scan-angle, as measured by the instrument, and the tangent height of the ray path through the atmosphere is considered. The instrument is unusual in that it scans in two opposite directions. This property is used to derive the scan angle from the same radiance profiles, which are used to determine the constituent profiles, subject only to the assumptions that the attitude is steady, the stratosphere is locally horizontally homogeneous, and the instrumental optical alignment is correct.

The results of this determination for the first flight of the Toronto Balloon Radiometer are compared to previous methods of determining the instrumental scan angle and are found to agree to the accuracy with which the comparisons are made. Techniques by which the accuracy and resolution of the two-sided attitude determination could be improved are discussed.

1. Introduction

Limb-scanning instruments are extremely useful for constituent profiling in the stratosphere by sensing thermal emission. The very long path length obtainable provides a substantial signal from gases in very low concentrations and, in contrast to a nadir view, the radiation input at the far end of the path is zero, and therefore only the atmospheric emission signal is seen. However the exact path observed depends critically on the angle-of-view. In order to determine the lowest point on the path, the "tangent height", to an accuracy of ±0.5 km at 15 km from a balloon at 40 km, the angle must be known to ±0.05°. This angle is conventionally measured from the horizontal, which is taken in this context to be the tangent to the average isobaric surfaces in the stratosphere.

There are many methods of measuring the orientation of a balloon package (magnetometers, gyroscopes), but these suffer from two major disadvantages for this application: They measure the position of the package rather than the optical beam, and they measure with reference to some parameter other than the atmosphere. Previous attempts to find the location of the "line-of-sight" in limb-scanning stratospheric sounders have been restricted to the satellite case and have concentrated on the interpretation of data from channels sensitive to CO_2 (Gille and House, 1971; Rodgers et al., 1984). The satellite problem is somewhat more complicated in that the temperature profile is unknown (but required for composition studies), whereas in the balloon case radiosonde data is readily available. The approach used in satellite instruments is to simultaneously retrieve a reference pressure level in the stratosphere and the temperature profile relative to the reference level, rather than attempting to find the absolute height of the "line-of-sight." The particular restrictions and flexibility of satellite systems lead to other operational variations and for more details the reader is referred to the papers already cited. We have attempted to resolve the problem for our balloon instrument by using the information contained in double-sided scanning data.

The simple technique of matching infrared emission signals from two directions to determine, or control, instrument attitude has previously been applied to satellite attitude control systems. The application of such a technique to balloon systems, particularly in a full two-sided system is, we believe, novel. The instrument is optimized for minor constituent profiling and thus neither its spectral passband, scanning nor field-of-view is ideal for attitude determination. However, the fact that we are using the same optical system, including the detector and electronics, for both measurements removes most of the uncertainty in the relative alignment of the attitude and scientific optical systems, as well as being a "free" addition to the instrument.

2. The Toronto balloon radiometer

The instrument itself is a limb-scanning pressure-modulator radiometer: however, the pressure-modulator property is not used in this discussion and the instrument can therefore be regarded as a simple limb-scanning radiometer with a spectral bandwidth of about 200 cm^{-1} centered at 1750 cm^{-1}. The complete instrument is an improved version of a previous instrument (Chaloner et al., 1978) used for measuring nitro-

© 1986 American Meteorological Society

Unauthenticated | Downloaded 06/25/24 07:09 PM UTC

gen oxides. The unusual feature of the current instrument is that it is a double-sided limb-scanner (Fig. 1) whose view is controlled by a single rotatable 45 degree mirror that has its rotation axis coincident with the beam axis (see Fig. 2). The double-sided scan was incorporated to allow the use of this attitude determination system and to allow the instrument to operate when one scan faced the sun and was therefore unusable because of reflections (the gondola is not rotationally stabilized at present and rotates freely). A shaft encoder on the mirror axle resolves the rotation of the scan mirror to 0.044 deg (13 bits of accuracy in a full shaft rotation). We currently have no indicator of compass direction apart from solar sensing thermistors in four quadrants. These indicate a form of slow rotation, but do not give the exact time evolution.

After the scanning mirror, the optical beam falls on a simple telescope consisting of a spherical mirror used in an off-axis system. Two steering mirrors are used to orientate and direct the beam through a rotating, reflecting chopper to the focal point. The reflecting chopper interrupts the beam at 760 Hz, alternating it with a view of a blackbody at 77 K in a dewar assembly above the chopper. At the first focus, the beam is refocused with a calcium fluoride lens and split into three fields by two mirrors. The instrumental field-of-view is defined by a slotted mask at this point to be 0.63 deg in the vertical and approximately 2.5 deg in the horizontal. The three optical beams then pass separately through the pressure-modulator cells and on to dewar assemblies containing the optical filters, a doublet germanium lens and finally the detector. This paper discusses data from the central channel, which is undeviated at the first focus. This channel is to be used for determination of formaldehyde concentrations using the 5.7 μm band. It will also sense some water vapor emission in the 6.3 μm band together with O_3 emission in the 5 μm band since these bands overlap with the formaldehyde band.

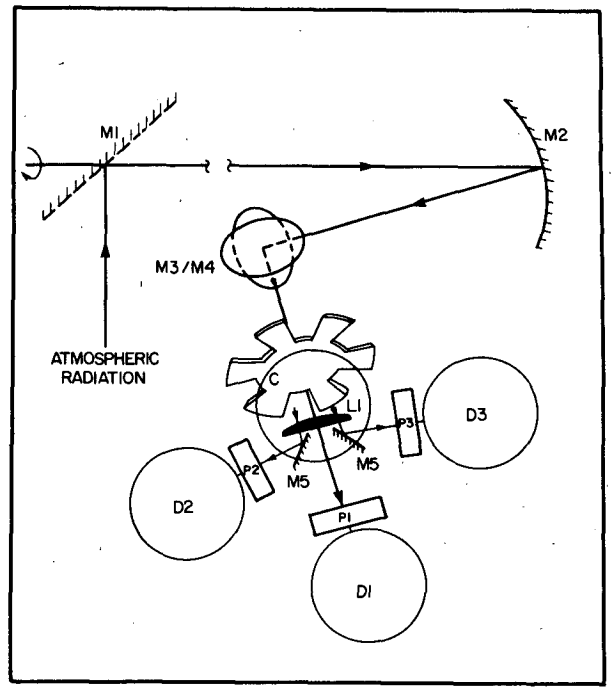

FIG. 2. Schematic (not to scale) of the main optical system of the Toronto Balloon Radiometer. Input radiation falls on M1, the scanning mirror and is then focused by M2 onto the field assembly L1/M5. Folding mirrors, M3/M4, rotate and steer the beam through the reflecting chopper C. From the field-splitting assembly, radiation passes into one of the three independent pressure modulator/detector channels (P1–P3, D1–D3) for measurement.

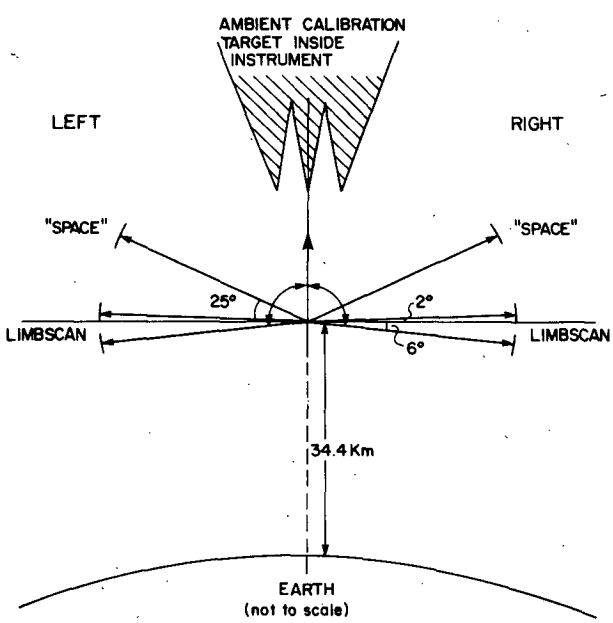

FIG. 1. Viewing geometry of the Toronto Balloon Radiometer. Scanning is controlled by a single rotatable mirror to allow viewing from both sides of the instrument of either the atmosphere, limb-scanning, or a "space" view, +25 deg to the horizontal for calibration zero. A central internal blackbody gives a second known radiance for the two-point calibration scheme.

Calibration is achieved by using an internal blackbody in front of the entire optical system, which provides a known radiance ("calibration" view), and from views at +25 deg for a radiation zero, ("space" view) as shown in Fig. 1. The radiative input to the instrument in space view is not exactly zero, but is sufficiently small to be considered zero in this discussion.

Typical radiometer-type signals for a left and right scan are shown in Fig. 3. These signals are almost entirely due to H_2O and O_3. Scanning is accomplished by stepping the mirror using a geared-down stepper-motor, which also drives the mirror to obtain calibration data. The part of the scanning mirror used remains invariant to first order during these rotations because of the system geometry, thereby assisting in the stability of the calibration. Scan steps were programmed to be

Unauthenticated | Downloaded 06/25/24 07:09 PM UTC

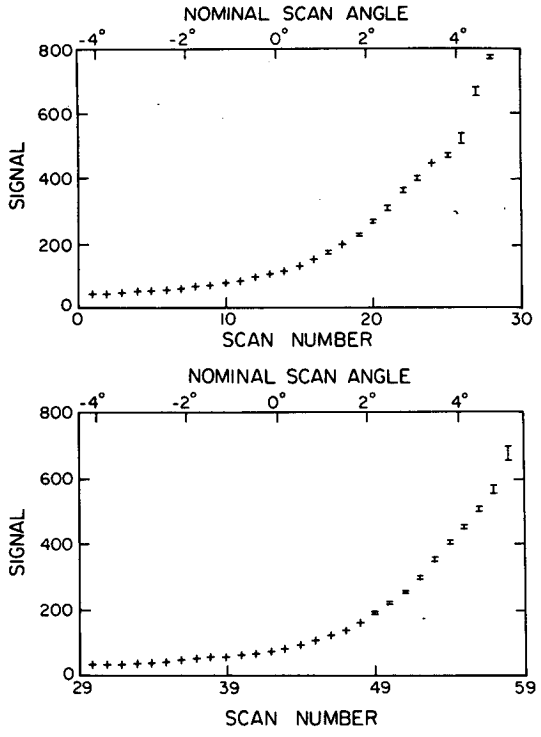

FIG. 3. Calibrated signals for a pair of left/right scans from the August 1983 flight record. The vertical scale is in units of μW m^{-2} sr^{-1} (cm^{-1})$^{-1}$. The "scan number" is a data tag for a particular scan point and larger numbers imply lower tangent heights. A scale of nominal scan angle (assuming $\gamma = 0$) runs along the top of each graph. The tropopause is visible in both scans as an increase in both signal and noise level. The error bars shown are the statistics from each set of 8 samples for a scan number. To determine the attitude, scans are overlaid and "slipped" against each other until a minimum in the sum of squared residuals is found (Fig. 5).

0.327 deg (two motor steps) for this flight. Subsequent flights may be able to use a step as small as 0.08 deg.

The instrument was flown for the first time from the National Research Council of Canada launch site in Gimli, Manitoba on 18 August 1983. Float altitude was maintained at 34.3 km for approximately 10 h, during which time data were continuously gathered. Two channels of the instrument were active for this flight, but the second one produced excessive detector noise, hence the data from this channel are of poor quality.

3. Scan theory

Since the scan position obtained using the shaft encoder is measured relative to the package (which is "leveled" before flight), we must assume that the package is stable during a complete scan sequence in order to be able to compare the two sets of data. Data from the first flight of the instrument suggests that this is so, and that the instrument does not swing, but does rotate with a period on the order of 2 hours. Assuming that the instrument is ideal, then the scans on both sides of the instrument should be identical, if the atmosphere is horizontally homogeneous.

The instrument views the atmosphere in a circular region up to 550 km from the package. Over that region the stratosphere is reasonably horizontally homogeneous in all physical parameters, particularly around the launch latitude and time (August 1983). In general the stratosphere is reasonably homogeneous, exhibiting only slow variations with distance except during warming events, which do not occur at this time of year in the Northern Hemisphere (Labitzke, 1980). From our data, we can find no evidence that indicates the resultant attitude is dependent upon azimuthal position, which would be evidence for a gradient. The tropopause, which is not horizontally homogeneous, is specifically excluded from this consideration.

In a limb-scanning instrument the signal comes primarily from the lowest levels of the path unless the constituent has a very steeply increasing mixing ratio with height. Water vapor, although not uniformly distributed in the stratosphere in the vertical direction (Harries, 1976; and Ellsaesser, 1983), apparently does not exhibit such extreme behavior and therefore our signal comes primarily from levels near the "tangent" or lowest height of the ray path. The concentration of water is, however, high enough that the observed spectrum may be considered to be a strong pressure-broadened spectrum of independent lines. It is true that there is some overlapping of the lines, but we may neglect this unless a detailed calculation is required. We can then assume, ignoring geometrical deviation from a full limb-path, that our signal is proportional to

$$B(\tilde{\nu}, T_t) \sum [\tau_f (S\alpha_0)^{1/2}](p_t u)^{1/2},$$

where B is the Planck function, $\tilde{\nu}$ the central wavenumber of the (narrow) band, T_t the tangent height temperature, $\tau_f(S\alpha_0)^{1/2}$ the root of the individual line-strength-halfwidth product multiplied by the instrument filter transmission, τ_f, at the line center, p_t is the tangent height pressure, and u is the total absorber amount. If we assume a constant H_2O mixing ratio in the atmosphere, then the total amount in the path is proportional to the tangent height pressure and the signal is approximately proportional to the product $B(\tilde{\nu}, T_t)p_t$. In the case of the O_3 band whose lines are much weaker we may use the weak line approximation:

$$B(\tilde{\nu}, T_t) \sum (\tau_f S)u,$$

where the symbols have the same meaning as above, and the pressure dependence is the same. These simple arguments will not suffice to calculate the signal exactly, but it will enable us to determine the degree to which inhomogeneity in the stratosphere, particularly in temperature, will affect the determination of the horizontal plane. Smaller contributions to the signal come from nitric acid (Rothman et al., 1981) and pressure-induced oxygen absorption (Rinsland et al., 1982), al-

Unauthenticated | Downloaded 06/25/24 07:09 PM UTC

though we are on the extreme edge of the latter band. Formaldehyde, although being sought in this experiment, does not contribute significantly to the observed radiance in this channel.

At 5.7 μm and 225 K, which are typical for the stratosphere, the Planck function changes by about 5% K^{-1} so that a temperature difference of 1 K between the two tangent points is equivalent to a pressure difference of 5% or a height difference of 0.3 km. For a 15 km tangent point, the angular error in determining the horizontal in the above case would be 0.015 deg. Thus a temperature error of the order of 2–3 K is required before our specified accuracy is exceeded. A temperature change of 3 K/10° of latitude is quite large for the situation we are considering, particularly when the spatial averaging property of a limb-path and the fact that balloon flights are only made in reasonably calm conditions is taken into account. Thus, in the absence of any contrary evidence as the package rotates, we may neglect temperature gradients.

Any differences between left and right scans are then attributed to instrumental effects, which may be the tilt of the package or asymmetry of the beam under rotation. The latter occurs if the optics are not truly axial and could be successfully eliminated by careful alignment, as will be discussed below.

We define α as the dip angle of the beam between the nominal horizontal and the true horizontal, and β, the beam asymmetry angle, as the excess angle by which the beam rotates when the mirror is rotated by exactly 180 deg. For a truly axial system, β will be zero but it can be nonzero for two reasons: First, if the beam is designed to be off-axis, as is the case for two of the channels; and second, if the optical alignment is imperfect. As stated above, the data discussed in this paper pertains to an on-axis system and therefore any nonzero value of β is due to optical misalignment.

If we select a case when the left and right signals are identical, the arguments concerning horizontal homogeneity presented above suggest that the true depression angles for the two cases are identical. If the true angle is θ and the measured angles for these cases are L and R, we find (Fig. 4) that:

$$\left.\begin{aligned} L &= \theta + \alpha \\ R &= \theta - \alpha - \beta \end{aligned}\right\}$$

or

$$L - R = 2\alpha + \beta = \gamma,$$

where γ is defined as the tilt angle.

Since α and β are constants for the scan we can improve the accuracy of the technique by comparing left and right scans using a least-squares technique for each scan. Using estimates from scan pairs throughout the flight, we can then estimate γ as a function of time. Care must be taken to eliminate data from the area of the tropopause and to weight the various estimates in

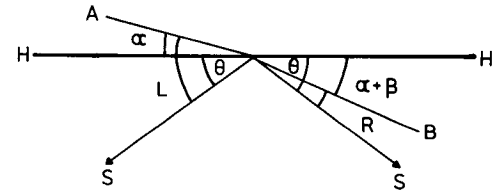

FIG. 4. Scanning with real offsets. The line H–H is the true horizontal and the lines A, B are the beam orientations when the shaft encoder indicates horizontal. The error is composed of two parts: the dip angle α, which is a measure of the package tilt, and the beam asymmetry angle β, which is the angular error in the beam between the two "horizontal" positions. The apparent angles L and R are the results of measurements at the true angle θ at which the left and right signals are equal. These measurements are affected by the dip angle and beam asymmetry angle, resulting in the equations for the apparent angles $L = \theta + \alpha$ and $R = \theta - \alpha - \beta$.

the scan appropriately. In this case, we minimize the function

$$\sum_j [S_L(k_j) - S_R(k_j + \gamma)]^2,$$

where S is the signal, k the nominal scan angle, subscripts L and R refer to left and right scans, respectively. The sum is done over a restricted range of scan positions. Data are interpolated between real data points using a linear formula. The sum of squares residuals after shifting the data of Fig. 3 is shown in Fig. 5 as a function of the angle γ and a definite minimum is found.

Each scan pair produces an estimate of γ and these are plotted as a function of time in Fig. 6. From these data, assuming $\beta = 0$, we find the dip angle to be: $\alpha = 0.35 \pm 0.03$ deg with no appreciable variation over the flight duration. Using this value for α, the true scan angles for individual measurements can now be absolutely determined. We have also examined the data for the other axial channel that shares the same optical system and detector. This channel uses the pressure modulator assembly but the signal is still almost entirely due to H_2O and O_3. The results show a very similar situation with a higher uncertainty, primarily due to the smaller signal-to-noise ratio in this channel. As mentioned earlier, it was not possible to evaluate the situation for the off-axis channel used in the first flight because of the excessive detector noise. It is hoped that future flights will be more successful in this regard.

4. Comparison with other data

In order to determine the accuracy of our method for determining attitude, it is necessary to compare it to another, independent calculation of the same quantity. A method used in the past (Drummond, 1977) has been to associate the abrupt increase in radiometric signal and noise level with the penetration of the instrumental field-of-view into the troposphere. If we can associate these features with the temperature discontinuity as measured by radiosonde ascents, then we

Unauthenticated | Downloaded 06/25/24 07:09 PM UTC

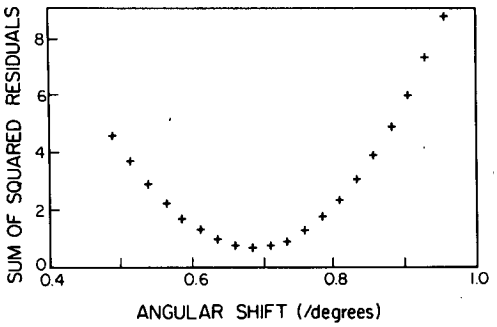

FIG. 5. Sum of squared residuals for the data of Fig. 3 as a function of γ. The vertical scale is in units of 10^{-9} [W m^{-2} sr^{-1} (cm^{-1})$^{-1}$]^2. A definite minimum can be seen at 0.68 deg and this forms one point on Fig. 6. Data from views near the tropopause are excluded from the summation as these are not expected to be similar for the two scans.

can determine the instrument attitude. There is, however, some uncertainty in the association of these two measurements as the signals seem to be influenced by stratospheric composition and dynamics as well as by the temperature profile. For example, the results of Kley et al. (1979) show that the water vapor concentration minimum sometimes occurs at a different height to the temperature minimum, leading to a possible confusion of a rapid signal rise with decreasing height due to increasing water vapor amount with a similar result due to rising temperature. In view of these facts it would not be surprising to see some systematic variations of several kilometers between the two estimates of tropopause height, with the height retrieved from the two-sided limb-scan probably overlying the estimate from radiosonde ascents. With the above facts in mind we have used these features to estimate tropopause height and thus validate our evaluation of the tilt angle and the accuracy of the optical alignment.

First considering the simultaneous increases in pressure, temperature and mixing ratio of water that occur below the tropopause, we expect to find a large rate of increase in the signal as the scan angle increases. This is in contrast to the lower stratosphere where the temperature and mixing ratios are more nearly constant with height. We would then expect to see a change of gradient in the signal as the tangent height moves down through the tropopause.

A plot of the signal for the "left" and "right" side of the instrument is shown in Fig. 7. For the left side we find that there is a discontinuity at scan position 27 which, assuming that the instrument tilt calculated in the last section is correct, corresponds to a tangent height of 11.5 km for this ray path. Position 26, with a tangent height of 14.6 km, has a lower bound on the field-of-view of 12.6 km. Although not evident in Fig. 7, a more detailed examination of all the individual scan datasets shows some evidence for the discontinuity at this level, but not a decisive change in all cases. The same analysis for the right scan data shows a very similar result.

Each mirror position is held for 8 seconds and the signal is sampled by the on-board computer every second; therefore each point in Fig. 7 is an average. Figure 8 shows the corresponding variances for the signals. If it is assumed that the lower stratosphere is reasonably

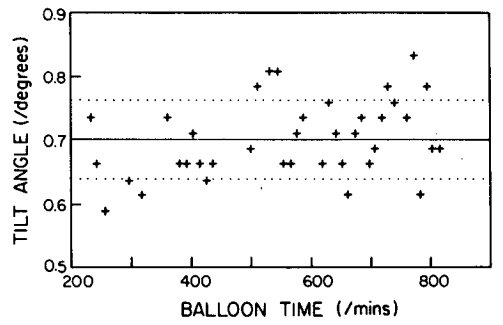

FIG. 6. Estimates of the tilt angle, γ, from the flight in August 1983 using 5.7 μm wideband channel data. The value for each point is found to a resolution of about ± 0.01 deg and is plotted without error bars as the variation in the estimates, from atmospheric "noise," forms the main error. The average value of γ, denoted by the solid line is 0.702 ± 0.06 deg taking the error as the statistical fluctuations in the individual estimates.

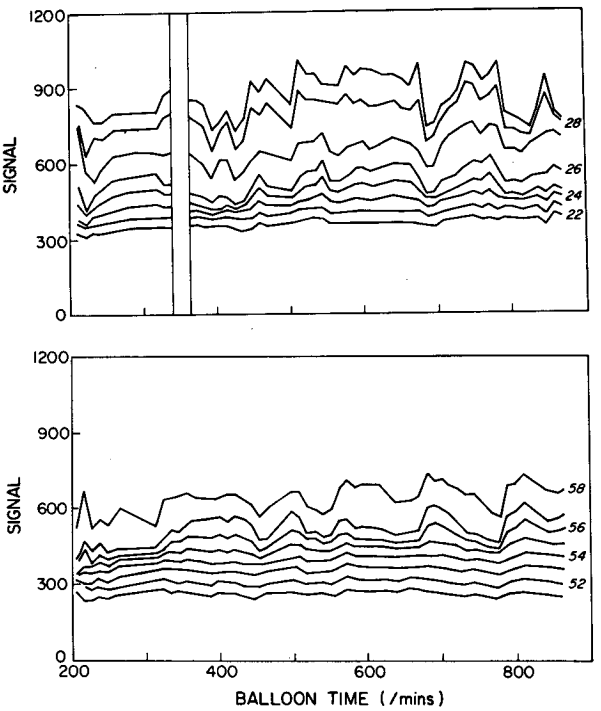

FIG. 7. Scan data for the lower tangent height views for the right and left scans plotted against time. The tropopause can be seen as a sudden change in the separation of the successive views, and can be seen between views 26–27 and 57–58. The vertical scale is in units of μW m^{-2} sr^{-1} (cm^{-1})$^{-1}$. The blank portion of the upper graph between the vertical lines (and Fig. 8) is where sun-glint produced erroneous calibration parameters.

Unauthenticated | Downloaded 06/25/24 07:09 PM UTC

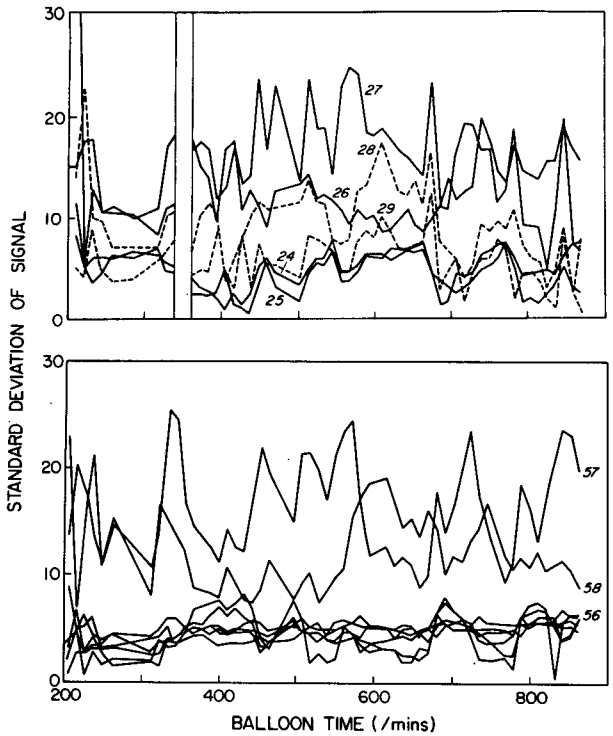

FIG. 8. The statistical errors in the signals shown in Fig. 7. The increased noise associated with views 26–27 and 57–58 can be clearly seen and is interpreted as evidence for the tropopause at this level. Views 28–29 have tangent heights below the tropopause and appear to have lower noise values again. The vertical scale is in units of μW m^{-2} sr^{-1} $(cm^{-1})^{-1}$.

uniform and that the tropopause and below are places of fairly rapid fluctuations, then the noise level would be expected to increase as the scan moves downward through the tropopause. Although this argument is somewhat tenuous, the noise level does seem to increase markedly at that level, an effect that has been noted in previous experiments (Drummond, 1977). Left views 26, 27 and 28 do show an excess noise, and on the right, views 57 and 58 are noisier than higher views. The noise level appears to decrease again as the tangent view moves into the lower troposphere as shown by views 28 and 29, where the noise level is decreasing.

As an example of an individual pair of scans showing the effects discussed before, we refer to Fig. 3. The increase in noise and signal are clearly visible in the left scan and less clearly in the right, due to the truncation of the scan just below the tropopause.

Based on this data, we can estimate the tropopause level to be between 11.5 and 14.6 km, or 13 ± 1.5 km, from the scan data. A scan at a higher angular resolution is required before we could reduce that error further. It should be noted that there is a small correction to these tangent heights in order to account for atmospheric refraction and that this lowers the average value by about 0.2 km. The total error range then corresponds to about ±0.17° in scan angle, which is well in excess of the error from the two-sided comparison.

Figure 9 shows the temperature profile at Gimli for three radiosonde ascents, before, on the day of, and after the flight. The three ascents are very similar, thus strengthening our argument that the stratosphere is uniform at this time and place. A tephigram analysis shows that the tropopause is at a level of 13 ± 1.5 km, which overlaps with the estimates derived above. This level is unusually high for the location and time. Examining data from surrounding sites for the time of flight and periods immediately before and after, revises this estimate to 12.5 ± 1.5 km, where the increased variation is due to site-to-site differences and the lack of precise azimuthal data from our instrument. Using this data, we conclude that the estimates of the tropopause from the balloon instrument and from the radiosondes are consistent, especially when the difficulties of reliably associating the temperature discontinuity and the radiance/noise changes are considered.

5. Discussion

We have shown that the two-sided attitude-sensing system produces an estimate of the local atmospheric horizontal, within the accuracy of the optical alignment and the homogeneity of the stratosphere, which is extremely accurate and consistent. By improving the instrument alignment by an accurate setup before, and

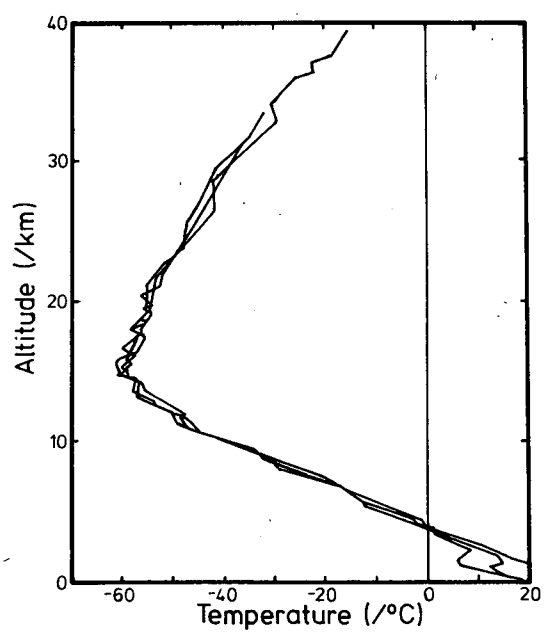

FIG. 9. An overlay of radiosonde ascents from Gimli, Manitoba, the launch site, for 1614 GMT 16 August, 1814 GMT 18 August and 1916 GMT 19 August 1983 (before and after flight time) showing a stable temperature profile in the lower and middle stratosphere. The tropopause level at this location appears to be stable at about 13 km. Other data show some variation in the tropopause height.

Unauthenticated | Downloaded 06/25/24 07:09 PM UTC

checking after, the flight, the confidence in this assessment can be increased. However, the arguments used to establish the tropopause level, although valid, are difficult to interpret in a high-resolution setting for a number of reasons. First, the finite field-of-view of the instrument makes it difficult to accurately assess the scan angle when the instrumental tangent height is at the tropopause level. Second, since the conditions at the tropopause vary in the horizontal as well as in the vertical, the exact form of the signal discontinuity at the tropopause is in doubt. Third, the measurement of tropopause level over a wide area cannot be accomplished to a very high accuracy, since this level varies. In light of this argument we have considered the question of accurate optical alignment of the instrument so that the beam rotation for a 180 deg mirror rotation, i.e. the angle β, is known to <0.1 deg. This is not a trivial operation as the whole alignment process must be done in the infrared rather than the visible, but it appears from calculations that a pair of Newtonian telescopes could be aligned to a sufficient accuracy to give a satisfactory approximation to a pair of plane parallel wavefronts approaching each other on a common axis. Inserting the instrument between these telescopes would allow a calibration of beam directions and shapes. The proposed experimental setup is shown in Fig. 10.

Using this equipment, the uncertainties in our method could be reduced considerably below those from methods using the temperature discontinuity near the tropopause, but without imposing the constraint that the beam direction relative to the package structure must be known.

This technique at first appears ideal for use in a satellite situation where the requirement for stability is even more severe and a common attitude/signal optical system is very desirable: for a 1000 km orbit a tilt angle or misalignment of 0.01 deg represents an error of 0.65 km in tangent height. However, the increased distance between the tangent points, now 60 deg in angular separation on the globe, implies that the arguments of homogeneity of the stratosphere cannot be applied. It may be possible to use a relatively simple model of stratospheric temperature to eliminate this effect, but this aspect of the problem has not been investigated. However, this system could form the basis of an optical attitude sensor for balloon systems using a fully or partially independent optical system. In this case a more suitable spectral region and bandwidth could be selected as well as better optimized scanning and instrumental field-of-view. It is intended to pursue this possibility in the future, along with refinements of the current technique.

6. Conclusions

We have demonstrated, using data from the first flight of the Toronto Balloon Radiometer, that it is possible to recover the balloon attitude to a high accuracy using the technique of two-sided limb-scanning. We believe that with appropriate refinement, which we are now actively investigating, this will produce data of a higher quality than previous attempts of balloon attitude recovery, with the advantage of measurements that use the same optical system as is used for the constituent profiling. A comparison of the new method with previous techniques shows that it is consistent with them, but has a higher potential for accurate measurements.

Acknowledgments. The Toronto Balloon Radiometer project is supported by grants from the Natural Science and Engineering Research Council of Canada and the Physics Department, University of Toronto. We would like to thank the workshop staff of the Department of Physics for their assistance with the instrument fabrication, the staff of ADGA systems for their support during the flight preparations of this instrument and the staff of the Canada Centre for Space Science for their assistance with instrument preparation and funding of the flight itself.

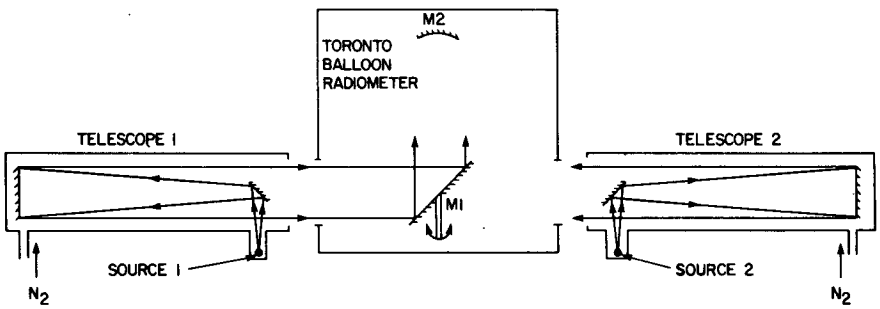

FIG. 10. Proposed experimental layout to measure field-of-view and optical alignment (angle β in the analysis) using two opposing telescopes. The telescopes provide two approaching plane parallel wavefronts of infrared radiation, which can be scanned from the instrument and correlated with the shaft encoder readings. Purge gas will be necessary in the telescopes to keep atmospheric water vapor absorption within reasonable limits, as will careful visual alignment using He–Ne lasers to ensure perfect focusing and a consistent optical axis.

Unauthenticated | Downloaded 06/25/24 07:09 PM UTC

REFERENCES

Chaloner, C. P., J. R. Drummond, J. T. Houghton, R. F. Jarnot and H. K. Roscoe, 1978: Infra-red measurements of stratospheric composition. I. The balloon instrument and water vapour measurements. *Proc. Roy. Soc. London,* **A364,** 145–159.

Drummond, J. R., 1977: Radiometric investigation of trace gases in the atmosphere. Ph.D. thesis, Clarendon Laboratory, Oxford, U.K., 303 pp.

Ellsaesser, H. W., 1983: Stratospheric water vapour. *J. Geophys. Res.,* **88(C6),** 3897–3906.

Gille, J. C., and F. B. House, 1971: On the inversion of limb radiance measurements. I: Temperature and thickness. *J. Atmos. Sci.,* **28,** 1427–1442.

Harries, J. E., 1976: The distribution of water vapour in the stratosphere. *Rev. Geophys. Space. Sci.,* **14,** 565–575.

Kley, D., E. J. Stone, W. R. Henderson, J. W. Drummond, W. J. Harrop, A. L. Schmeltekopf, T. L. Thompson and R. H. Winkler, 1979: In-situ measurements of the mixing ration of water vapor in the stratosphere. *J. Atmos. Sci.,* **36,** 2513–2524.

Labitzke, K., 1980: Climatology of the stratosphere and mesosphere. *Phil. Trans. Roy. Soc. London,* **A296,** 7–18.

Rinsland, C. P., M. A. H. Smith, R. K. Seals, Jr., A. Goldman, D. G. Murcray, J. C. Larsen and P. L. Rorig, 1982: Stratospheric measurements of collision-induced absorption by molecular oxygen. *J. Geophys. Res.,* **87(C4),** 3119–3122.

Rodgers, C. D., R. L. Jones and J. J. Barnett, 1984: Retrieval of temperature and composition from NIMBUS 7 SAMS. *J. Geophys. Res.,* **89(D4),** 5280–5286.

Rothman, L. S., A. Goldman, J. R. Gillis, R. H. Tipping, L. R. Brown, J. S. Margolis, A. G. Maki and L. D. G. Young, 1981: AFGL Trace Gas Compilation: 1980 version. *Appl. Opt.* **20,** 1323–1328.

Unauthenticated | Downloaded 06/25/24 07:09 PM UTC